Kinetic Characterization of CheY Phosphorylation Reactions: Comparison of P-CheA and Small-Molecule Phosphodonors†

Todd L. Mayover,‡ Christopher J. Halkides,§ and Richard C. Stewart*,‡

Department of Cell Biology & Molecular Genetics, University of Maryland, College Park, Maryland 20742, and Department of Chemistry, University of North Carolina−Wilmington, Wilmington, North Carolina 28403

Received July 16, 1998; Revised Manuscript Received December 22, 1998

ABSTRACT: In the chemotaxis system of *Escherichia coli*, phosphorylation of the CheY protein plays an important role in regulating the swimming pattern of the cell. In vitro, CheY can be phosphorylated either by phosphotransfer from phospho-CheA or by acquiring a phosphoryl group from any of a variety of small, high-energy phosphodonor molecules such as acetyl phosphate. Previous work explored the rapid kinetics of CheY phosphorylation by CheA. Here we extend that work and examine the kinetics of CheY phosphorylation by several small-molecule phosphodonors, including acetyl phosphate, benzoyl phosphate, carbamoyl phosphate, 2-methoxybenzoyl phosphate, and phosphoramidate. Our results indicate that these phosphodonors bind to CheY with relatively low affinity (K_s values ranging from 10 to 600 mM) and that the rate constant (k_{phos}) for phosphotransfer at saturating phosphodonor concentrations is relatively slow (values ranging from 0.05 to 0.5 s^{-1}). By contrast, under identical conditions, phosphorylation of CheY by phospho-CheA occurs much more rapidly ($k_{phos} \sim 800$ s^{-1}) and reflects CheY binding to phospho-CheA considerably more tightly ($K_s \sim 60$ μM) than it does to the small-molecule phosphodonors. In comparing CheA-mediated phosphorylation of CheY to small-molecule-mediated phosphorylation of CheY, the large difference in k_{phos} values suggests that phospho-CheA makes significant contributions to the catalysis of CheY phosphorylation. The effects of pH and ionic strength on CheY phosphorylation kinetics were also investigated. For CheA→CheY phosphotransfer, increasing ionic strength resulted in increased K_s values while k_{phos} was unaffected. For CheY phosphorylation by small-molecule phosphodonors, increasing ionic strength resulted in decreasing K_s values and increasing k_{phos} values. The significance of these effects is discussed in relation to the catalytic mechanism of CheY phosphorylation by phospho-CheA and small-molecule phosphodonors.

Escherichia coli, *Salmonella typhimurium*, and many other bacteria move through liquid environments by swimming, an ability that results from rotation of their flagella (*1*−*5*). These swimming cells accomplish chemotaxis (directed movement) by controlling how often they change direction as they move through environments containing gradients of attractant and repellent chemicals (*4*−*9*). CheY participates in this system (*10*−*12*) by binding to the 'switch' component of the flagellar motor (*13*). This interaction modulates the direction of flagellar rotation (CW versus CCW[1]) (*14*, *15*), and this determines whether a cell continues swimming in the current direction (CCW motor rotation) or changes direction by 'tumbling' (CW motor rotation). Phosphorylation of CheY at Asp^{57} regulates the ability of this protein to bind to the flagellar switch (*16*, *17*). Phosphorylated CheY (P-CheY) binds tightly to the switch, while unphosphorylated CheY binds relatively weakly (*13*, *18*). Consequently, the ability of P-CheY to promote CW flagellar rotation is about 100 times the corresponding activity of unphosphorylated CheY (*15*).

Phosphorylation of CheY is directed by CheA, an autophosphorylating histidine protein kinase (*19*, *20*). CheA, in turn, is regulated by the chemotaxis receptor proteins (*21*−*23*). CheA autophosphorylates (on His^{48}) utilizing the γ-phosphoryl group of ATP. P-CheY is then generated as a result of phosphotransfer from His^{48} of P-CheA to Asp^{57} of CheY (*16*, *24*, *25*). The lifetime of P-CheY is relatively short. CheY readily autodephosphorylates ($t_{1/2} \sim 15$−20 s) without the assistance of any other proteins (*24*, *25*). SDS-denatured P-CheY has a half-life of several hours (at neutral pH), typical for an acyl phosphate (*26*), and so it appears that native P-CheY catalyzes its own dephosphorylation. Another component of the signaling pathway, CheZ, serves as a CheY phosphatase and can further reduce the half-life of P-CheY by several orders of magnitude (*27*−*29*). Therefore, in any in vivo or in vitro situation, the ratio of P-CheY to unphosphorylated CheY is determined by the relative rates of phosphorylation and dephosphorylation.

The CheA−CheY sensory response circuit is one of the best characterized examples of a 'two-component system',

† This research was supported by U.S. Public Health Service Grant GM52583 to R.C.S.

* Corresponding author. Phone: (301) 405-5475. FAX: (301) 314-9489. Email: rs224@umail.umd.edu.

‡ University of Maryland.

§ University of North Carolina−Wilmington.

[1] Abbreviations: AcP, acetyl phosphate; bis-tris propane, 1,3-bis-[tris(hydroxymethyl)methylamino]propane; CHES, 2-(*N*-cyclohexylamino)ethanesulfonic acid; CCW, counterclockwise; CW, clockwise; MES, 2-(*N*-morpholino)ethanesulfonic acid; P-CheA, phosphorylated CheA; P-CheY, phosphorylated CheY; P_i, inorganic phosphate.

10.1021/bi981707p CCC: $18.00
Published on Web 02/05/1999

a type of signal transduction circuit that is utilized in a wide variety of organisms to mediate an array of different kinds of responses (*30*, *31*). In each two-component system, the activity of a response regulator protein (a CheY homolog) is controlled via phosphorylation by a cognate sensor kinase (a CheA homolog). CheY is one of the best characterized members of the response regulator superfamily. Crystal structures of various forms of the protein (*32*−*34*) and an NMR-derived structure (*35*) have been reported. CheY and other response regulators can become phosphorylated not only by interacting with their cognate sensor kinases but also by acquiring a phosphoryl group from a variety of high-energy phosphodonor molecules, such as acetyl phosphate, in the absence of any kinase (*26*, *36*−*39*). Some of these small-molecule phosphodonors are generated by metabolic pathways in the bacteria and, therefore, have the potential to affect response regulator activity in vivo (*37*). In vitro, CheY can acquire a phosphoryl group from any of a wide array of structurally distinct high-energy phosphodonor molecules including many, but not all, acyl phosphates, phosphoramidate, and phosphoimidazole (*26*, *36*, *40*). Phosphorylation of CheY by such small-molecule phosphodonors and CheY phosphorylation by CheA both result in phosphorylation of Asp^{57} of CheY, and both require participation of a divalent metal ion, such as Mg^{2+} (*24*, *26*, *27*, *39*).

In the work reported here, we investigated the kinetics of CheY phosphorylation by several different small-molecule phosphodonors, and we examined the effects of ionic strength and pH on this reaction. We compared these results to those obtained from similar kinetic characterization of the CheA→CheY phosphotransfer reaction (*41*). This information serves several useful purposes: (i) it enables assessment of whether CheY phosphorylation by small-molecule phosphodonors is expected to contribute significantly to generation of P-CheY in vivo; (ii) it provides some insight into the catalytic mechanism of CheY phosphorylation by small-molecule phosphodonors and how the basic chemistry of this reaction might be accelerated in the context of the CheA·CheY complex; (iii) it provides basic kinetic information that should prove useful for experiments in which P-CheY is generated using small-molecule phosphodonors.

EXPERIMENTAL PROCEDURES

Protein Preparations. Published methods (*42*) were used to overproduce and purify *E. coli* CheY and CheA. CheY and CheA protein concentrations were determined spectrophotometrically using extinction coefficients (8.25 mM^{-1} cm^{-1} for CheY, 16.3 mM^{-1} cm^{-1} for CheA) calculated by the method of Gill and von Hippel (*43*). $CheA^{124-257}$ was purified from strain RP3098 carrying plasmid pTM22 following the procedures of Morrison and Parkinson (*44*). Protein concentrations of $CheA^{124-257}$ samples were determined using the BCA assay kit from Pierce Chemical Co.. Phosphorylated CheA (P-CheA) was generated as described previously (*25*) except that nonradioactive ATP was used. Control experiments using [γ-^{32}P]ATP under identical conditions indicated that ∼50% of the CheA was phosphorylated.

Chemicals. Acetyl phosphate (potassium, lithium salt) and carbamoyl phosphate (disodium salt) were purchased from Sigma. Analysis of these chemicals (*45*) for acyl phosphate content indicated purities of ∼90%, and the phosphodonor concentrations reported here have been corrected to reflect this. Benzoyl phosphate (*46*), 2-methoxybenzoyl phosphate (*47*), and the potassium salt of phosphoramidate (*48*) were synthesized and characterized using published methods. The purities of these phosphodonors were as follows: 60−75% for two different benzoyl phosphate preparations [based on acyl phosphate content (*45*) and UV absorbance spectrum]; 80−95% for two different preparations of potassium phosphoramidate (based on ^{31}P-NMR); and 70−90% for different fraction pools from a single preparation of 2-methoxybenzoyl phosphate (based on acyl phosphate content and UV absorbance spectrum). Appropriate corrections were made in calculating the concentrations of these phosphodonors reported here. Further analysis of the phosphodonor preparations indicated that the contaminants were hydrolysis products. Thus, acetyl phosphate solutions contained 10% acetate and phosphate, benzoyl phosphate contained 25−40% benzoic acid and phosphate, etc. We tested such contaminants (acetate, phosphate, benzoate, ammonium acetate) for possible inhibition of CheY phosphorylation and observed no significant effects on the rate of reaction of CheY with 10 mM acetyl phosphate (potential inhibitors present at 50 and 100 mM, ionic strength maintained at 0.3 M). Similar experiments were carried out using hydrolysis products generated by subjecting phosphodonor solutions to acid-catalyzed hydrolysis. These solutions (following neutralization) did not affect CheY phosphorylation by 10 mM acetyl phosphate (results not shown).

Stopped-Flow Fluorescence and Absorbance Measurements. Time courses for CheY phosphorylation reactions were monitored by following the decrease in intrinsic fluorescence of CheY that results from its phosphorylation (*36*). CheY was mixed with various phosphodonor substrates in an Applied Photophysics SX.17MV stopped-flow spectrofluorometer (deadtime ∼2 ms). The resulting reaction mixtures were maintained at 24−25 °C in the thermostated observation chamber of the instrument (path length 0.2 cm). For fluorescence measurements, samples were excited at 295 nm (4 nm slit width on the excitation monochromator), and fluorescence emission was monitored either at 346 nm (making use of an emission monochromator with 5 nm slit width) or at a combination of wavelengths >335 nm (making use of a cutoff filter). Unless specified otherwise, all reactions were carried out in TMD buffer (50 mM Tris-HCl, 10 mM $MgCl_2$, 0.5 mM DTT, pH 7.5) containing KCl at a concentration required to reach the desired ionic strength. Observed rate constants were obtained by fitting each time course to a single exponential using the least-squares curve-fitting function of the SX.17MV work station [Marquart algorithm based on the Curvefit routine of Bevington (*49*)]. In fitting time courses observed for phosphotransfer from P-CheA to CheY, such fits included only data collected after the deadtime of the instrument (2 ms).

UV absorbance measurements to assay steady-state rates of consumption of benzoyl phosphate and 2-methoxybenzoyl phosphate were also made in the SX.17MV stopped-flow instrument. In analyzing the observed absorbance changes, we used $\Delta\epsilon_{285\ nm} = 0.6\ mM^{-1}\ cm^{-1}$ for conversion of benzoyl phosphate to benzoate and $\Delta\epsilon_{301\ nm} = 2.7\ mM^{-1}\ cm^{-1}$ for conversion of 2-methoxybenzoyl phosphate to 2-methoxybenzoate. These $\Delta\epsilon$ values were measured directly

in the stopped-flow observation chamber and agree with previously published values (*46*, *47*).

At high concentrations (e.g., above 100 mM), most of the phosphodonors used in this work began to slowly precipitate if 10 mM Mg^{2+} was added. To avoid complications arising from this, we prepared phosphodonor solutions in the absence of Mg^{2+} and set the $MgCl_2$ concentration in the CheY solution at 20 mM so that the final Mg^{2+} concentration in the stopped-flow reaction mixes would be 10 mM. Under these conditions, precipitation of phosphodonors was noticeable only on a time scale of many minutes after mixing. By contrast, the phosphorylation reactions were complete within 50−100 s and so were not affected by the very slow precipitation.

Model for Analysis of Kinetic Results. We analyzed our results using the following basic reaction scheme:

$$\text{CheY} \underset{k_{-1}}{\overset{A\sim P,\ k_1}{\rightleftharpoons}} \text{CheY}\cdot\text{A}\sim\text{P} \xrightarrow{k_{phos}} \text{P–CheY} \xrightarrow{k_{dephos}} \text{CheY} \qquad (1)$$

(A: dephosphorylated donor; P_i: inorganic phosphate)

in which A∼P represents the phosphodonor molecule (e.g., P-CheA or acetyl phosphate) and A represents the dephosphorylated version of the phosphodonor (e.g., CheA or acetate). To monitor phosphotransfer from P-CheA to CheY, we maintained [CheY] > 8 × [P-CheA] to ensure pseudo-first-order conditions. Under such conditions, the following equation relates the observed rate constant to the rate constants for the individual steps in the scheme above (*50*):

$$k_{obs} = \frac{k_1 k_{phos}[\text{CheY}]}{k_{-1} + k_1[\text{CheY}]} + k_{dephos} \qquad (2)$$

However, previous work (*41*) and results reported here indicated that k_{dephos} makes a negligible contribution and can be disregarded (i.e, phosphorylation of CheY by P-CheA is much more rapid than CheY dephosphorylation and so its contribution to the rate of approach to steady state can be ignored). This equation indicates that plots of k_{obs}^{-1} versus $[\text{CheY}]^{-1}$ will have a *y*-axis intercept equal to k_{phos}^{-1} and that K_S^{P-CheA} (the dissociation constant for the P-CheA·CheY complex) will be indicated by the ratio of the slope to the *y*-axis intercept (or the reciprocal of the *x*-axis intercept).

For monitoring phosphorylation of CheY by acetyl phosphate (and other small-molecule phosphodonors) to CheY, we set [AcP] > 500 × [CheY] to ensure pseudo-first-order conditions. Under such conditions, the following equation relates the observed rate constant to the rate constants for the individual steps in the scheme above (*50*):

$$k_{obs} = \frac{k_1 k_{phos}[\text{AcP}]}{k_{-1} + k_1[\text{AcP}]} + k_{dephos} \qquad (3)$$

Unlike the A→Y phosphotransfer reaction, phosphorylation of CheY by AcP is relatively slow, and so the k_{dephos} term cannot be considered to be negligible. The relationship described in eq 3 predicts that k_{obs} will reach a limiting value at saturating phosphodonor concentration, but that plots of k_{obs}^{-1} versus $[\text{AcP}]^{-1}$ will become nonlinear at low AcP concentrations, reaching a limiting value at which k_{obs}^{-1} equals k_{dephos}^{-1} (*50*). This prediction is borne out in our results (Figure 2A). According to eq 3, a plot of $(k_{obs} - k_{dephos})^{-1}$ versus $[\text{AcP}]^{-1}$ will be linear with a *y*-axis intercept equal to $(k_{phos})^{-1}$, and the ratio of the slope of this plot to its *y*-axis intercept will define the dissociation constant (K_s) of the CheY·AcP complex (k_{-1}/k_1). Although presented here for the specific case of AcP, we found that the same basic reaction scheme and analysis were appropriate for the reaction of CheY with the other small-molecule phosphodonors described in this report.

The reaction scheme presented in eq 1 is the simplest one that can account for all of our experimental observations. We ruled out several alternative models because they were at odds with our results. For example, we ruled out the possibility that the reaction between CheY and acetyl phosphate is a simple second-order reaction (without any detectable Michaelis complex) because of our observation that k_{obs} reaches a limiting value at sufficiently high acetyl phosphate concentrations. We also considered the possibility that this limiting rate reflected a rate-limiting conformational change in CheY (e.g., converting it from a phosphorylation-incompetent state to a phosphorylation-competent conformation). However, in such a situation the value of the limiting rate constant is expected to be the same for all small-molecule phosphodonors, a prediction that is not borne-out by our results (Table 1).

RESULTS

Effect of Phosphodonor Concentration on CheY Phosphorylation Kinetics. The intrinsic fluorescence of CheY decreases considerably upon phosphorylation of Asp^{57}, presumably reflecting the corresponding change in the electronic environment of the lone tryptophan residue (Trp^{58}) of CheY (*36*). Using a stopped-flow spectrofluorometer, we followed the time course of this fluorescence decrease after CheY was mixed rapidly with several different phosphodonors: acetyl phosphate (AcP), potassium phosphoramidate, carbamoyl phosphate, and benzoyl phosphate. As illustrated in Figure 1A for AcP, CheY intrinsic fluorescence decreased in an exponential manner after mixing, and then ultimately reached a plateau. Previous work established that this plateau reflects a steady-state situation in which the rate of CheY phosphorylation equals the rate of CheY autodephosphorylation (*36*, *40*). Each of the fluorescence time courses we recorded followed a single-exponential decay for more than five half-lives, as indicated by the linearity in semilog plots such as Figure 1B. We observed no evidence of biphasicity, burst kinetics, or lags. Similar single-exponential decreases were observed with potassium phosphoramidate, carbamoyl phosphate, and benzoyl phosphate (results not shown). With methoxybenzoyl phosphate, the relatively intense fluorescence of the substrate precluded attempts to focus on the CheY fluorescence signal. Our results (Figure 1) indicated that the rate of approach to the steady state (k_{obs}) and the magnitude of the observed fluorescence change (ΔF_{obs}) at steady state were sensitive to the concentration of phosphodonor.

By monitoring CheY fluorescence changes, we studied the time courses for the approach to steady state when CheY was mixed with these different phosphodonors over a range of concentrations. Analysis of these results enabled us to estimate the dissociation constant (K_s) for each CheY· phosphodonor complex and to define the value of k_{phos}, the

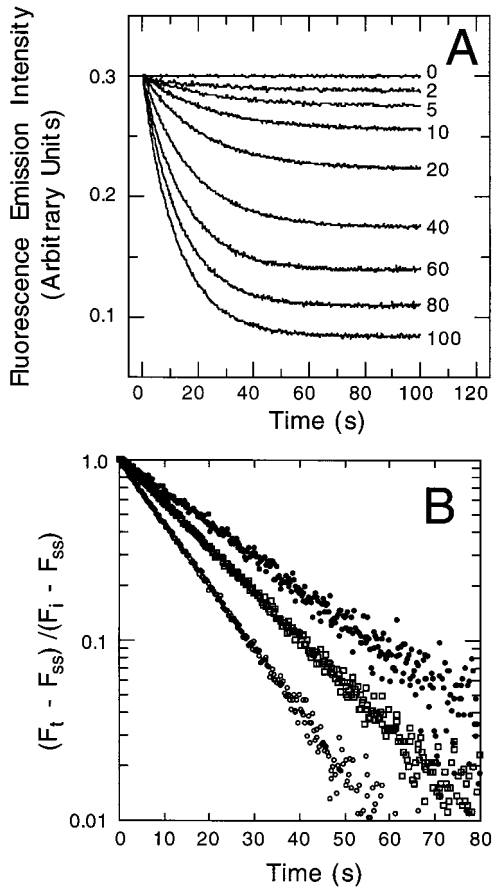

FIGURE 1: Time course of CheY phosphorylation monitored by fluorescence. CheY (2 μM final concentration) was mixed with acetyl phosphate at the indicated concentrations (mM) in a stopped-flow spectrofluorometer. Ionic strength was balanced at 1.6 M by addition of KCl. Panel A: CheY fluorescence emission intensity was monitored for 50−100 s after initiating each reaction (by mixing). Each time course represents the average of data generated by 5 consecutive 'shots'. (B) semilog plots of some of the data from panel A: (●) 5 mM AcP; (□) 40 mM AcP; (○) 100 mM AcP. Such plots are linear for over 5 half-lives, indicating that time course are fit very well by single exponentials and that there is no indication of lags or burst kinetics. F_t is the fluorescence emission intensity at time t, F_{ss} is the final fluorescence intensity reached at steady state; F_i is the fluorescence emission intensity at $t = 0$.

rate constant for the phosphotransfer step within each CheY·phosphodonor complex. Such analysis required that we assume a specific model for the phosphorylation reaction mechanism. This model is described in detail under Experimental Procedures and represents the simplest scheme that can account for our experimental observations. In the following paragraph, we describe our analysis of the results we obtained monitoring the reaction of CheY with AcP. The same experimental approach and analysis were applied in studying CheY phosphorylation by phosphoramidate, carbamoyl phosphate, and benzoyl phosphate. For these phosphodonors, we have not provided detailed descriptions of the data, but rather have summarized our findings in Table 1.

The dependence of k_{obs} on AcP concentration indicated that the phosphorylation reaction reached a saturating value at high [AcP], but a double-reciprocal plot of these data (k_{obs}^{-1} versus $[AcP]^{-1}$) exhibited pronounced curvature at high values of $[AcP]^{-1}$. Such curvature is expected for a situation in which k_{obs} is influenced not only by the rate of CheY phosphorylation but also by the rate of CheY autodephosphorylation (eq 3). Extracting useful information about the rate of CheY phosphorylation from the k_{obs} values required secondary treatment of the data to correct for the effects of dephosphorylation kinetics. This treatment involved simply subtracting k_{dephos} from each k_{obs} value (*50*). As predicted by eq 3, a plot of $(k_{obs} - k_{dephos})^{-1}$ versus $[AcP]^{-1}$ is linear (Figure 2B), indicating that the rate of CheY phosphorylation exhibits a hyperbolic dependence on AcP concentration. According to eq 3, the *y*-axis intercept of Figure 2B defines k_{phos}^{-1}, and the ratio of the slope of this line to the *y*-axis intercept defines the dissociation constant (K_s) of the CheY·AcP complex. The values of k_{phos} and K_s for the reaction of CheY with AcP are shown in Table 1. These values are averages from 3 independent determinations. Similar analysis was used to determine the K_s and k_{phos} values for the reaction of CheY with phosphoramidate, carbamoyl phosphate, and benzoyl phosphate.

Table 1: Dissociation Constants and Phosphotransfer Rate Constants for CheY·Phosphodonor Complexes at $I = 1.6$ M

phosphodonor	k_{phos} (s^{-1})	K_s (mM)
P-CheA[a]	800 ± 200	0.060 ± 0.03
acetyl phosphate[a]	0.08 ± 0.02	60 ± 25
phosphoramidate[a]	0.4 ± 0.1	400 ± 150
carbamoyl phosphate[a]	0.48 ± 0.14	600 ± 200
benzoyl phosphate[a]	0.07 ± 0.02	16 ± 6
benzoyl phosphate[b]	0.06 ± 0.02	20 ± 5
2-methoxybenzoyl phosphate[b]	0.10 ± 0.02	12 ± 6

[a] Values determined from experiments monitoring kinetics of CheY fluorescence changes. [b] Values determined from experiments monitoring substrate consumption using absorbance changes.

For the results presented in Figure 2B and Table 1, the value of k_{dephos} we used for correction of our k_{obs} values was 0.034 s^{-1}. This value can be obtained by extrapolating plots of k_{obs} versus [phosphodonor] to the *y*-axis; i.e., such plots have a nonzero *y*-axis intercept that defines k_{dephos} (see Figure 2A inset and eq 3) (*50*). Such extrapolations can be difficult because they rely on data obtained at very low phosphodonor concentrations, where the steady-state level of CheY−P is low: the resulting change in fluorescence signal is correspondingly small, and the experimental uncertainty in k_{obs} is comparatively large. Using this extrapolation approach, we obtained k_{dephos} values ranging from 0.030 to 0.040 s^{-1} for a variety of different experiments with each of the different phosphodonors. Thus, we saw no evidence that k_{dephos} was affected by the nature of the phosphodonor. A more accurate estimate of k_{dephos} was obtained in the pH−jump experiment described below. This value was 0.034 s^{-1} under the conditions used for the experiments summarized in Table 1.

CheY Phosphorylation Kinetics Monitored by Substrate Turnover. Two of the phosphodonor molecules studied here (benzoyl phosphate and 2-methoxybenzoyl phosphate) undergo small changes in the UV absorbance spectrum when they donate their high-energy phosphoryl group to CheY (or any other phosphoacceptor) (*46*, *47*). By following these absorbance changes, we monitored the steady-state turnover of these substrates by CheY in the presence and absence of CheZ. Results obtained with benzoyl phosphate are summarized in Figure 3. In the absence of CheZ, the CheY turnover number (V_{max}) is expected to be limited significantly

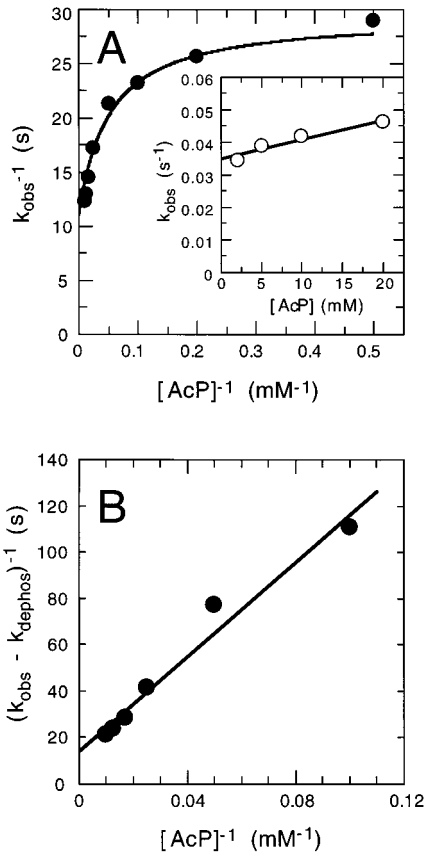

FIGURE 2: Effect of acetyl phosphate concentration on the rate of approach to the steady-state level of P-CheY. The observed rate constant for the exponential approach to steady (k_{obs}) was determined for the reaction of CheY (2 μM) with acetyl phosphate at a range of concentrations (2−100 mM) as in Figure 1. Ionic strength was balanced at 1.6 M using KCl. k_{obs} values were determined by least-squares fitting of each time course to a single exponential. (A) Plot of k_{obs}^{-1} as a function of $[AcP]^{-1}$ indicating that k_{obs} reaches a limiting value at saturating acetyl phosphate concentrations. In addition, as shown in the inset, at very low acetyl phosphate concentrations there is a linear relationship between k_{obs} and [AcP] that can be extrapolated to define a nonzero *y*-axis intercept (0.034 s^{-1}). (B) Reciprocal plot resulting from secondary treatment of the data in panel A to correct for the effect of CheY autodephosphorylation, as discussed in the text. The solid line represents the best linear fit to the data and indicates a *y*-axis intercept of 14.0 s and a slope of 1025 s mM.

by the rate of CheY autodephosphorylation, and the K_m value defined by a Lineweaver−Burk plot (Figure 3, open circles) does not directly indicate K_s, but rather a value related to K_s by the expression: $K_m = K_s k_{dephos}/(k_{phos} + k_{dephos})$. Our results indicated a turnover number of ~0.03 s^{-1} and a K_m of ~8.5 mM for CheY-mediated turnover of benzoyl phosphate in the absence of CheZ. In the presence of CheZ, the rate of CheY dephosphorylation is enhanced considerably (*25*−*29*). Therefore, when we allowed CheY to turn over benzoyl phosphate in the presence of excess CheZ, the CheY phosphorylation reaction was rate-limiting. Under these conditions, the K_m and extrapolated turnover number indicated in Figure 3 (closed circles) reflect K_s and k_{phos}, respectively. These values, reported in Table 1, match very well with those determined independently by monitoring CheY fluorescence changes. This agreement verifies that the kinetic parameters derived from analysis of the kinetics of CheY fluorescence changes accurately reflect the kinetics of substrate turnover. Steady-state turnover of 2-methoxybenzoyl phosphate by CheY can be monitored in a similar manner (Stephan Schuster, personal communication), and our analysis of these results defined the K_s and k_{phos} values shown in Table 1.

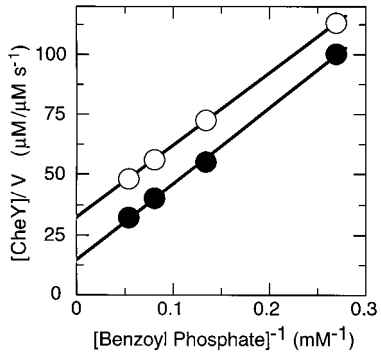

FIGURE 3: Analysis of steady-state turnover of benzoyl phosphate by CheY. CheY (20 μM final concentration) was mixed with benzoyl phosphate at concentrations ranging from 1.2 to 20 mM in TM buffer containing KCl to balance ionic strength at 1.6 M. Turnover of the benzoyl phosphate was monitored by following the decrease in absorbance at 285 nm. Reactions were carried out in the 0.2 cm observation chamber of a stopped-flow spectrophotometer. (○) Results obtained in the absence of CheZ; (●) results obtained in the presence of 4 μM CheZ. The lines represent the best linear fits to the data. In the absence of CheZ, this fit indicated a *y*-axis intercept of 33 s and a slope of 280 s mM. In the presence of CheZ, the best linear fit gave a *y*-axis intercept of 15 s and a slope of 310 s mM.

Ionic Strength Dependence of CheY Phosphorylation by Small-Molecule Phosphodonors. The concentrations of phosphodonor required to reach maximal k_{obs} [or to define the maximal ΔF_{obs}, as in previous work (*36*, *40*)] are relatively high and impart a correspondingly high ionic strength to the reaction mixture. The experiments reported above were performed at a balanced ionic strength (I =1.6 M) that enabled us to explore a large range of phosphodonor concentrations. We examined the effect of ionic strength on the kinetics of CheY phosphorylation by monitoring the time course of CheY fluorescence changes following addition of a fixed concentration of phosphodonor to CheY solutions in the presence of a range of salt concentrations. Our results indicated that increasing salt concentrations caused a significant decrease in the observed rate of approach to steady state (Figure 4A,B). This same effect was observed in experiments using three different salt species (potassium chloride, potassium glutamate, and sodium chloride) and was not diminished by doubling the $MgCl_2$ concentration (from 10 mM to 20 mM). Therefore, the effect of salt concentration on CheY phosphorylation kinetics appears to reflect sensitivity to ionic strength rather than specific binding of salt ions to CheY or weak chelation of Mg^{2+} by anionic components of the salt solutions. The results in Figure 4A,B demonstrated the magnitude of the effect for two different phosphodonors (acetyl phosphate and phosphoramidate); ionic strength effects were also observed with benzoyl phosphate, methoxybenzoyl phosphate, and carbamoyl phosphate (results not shown).

In theory, the effects shown in Figure 4A,B could have resulted from ionic strength influencing the rate of CheY phosphorylation, the rate of CheY dephosphorylation, or some combination of both. To explore the possibility that ionic strength affected CheY dephosphorylation, we took

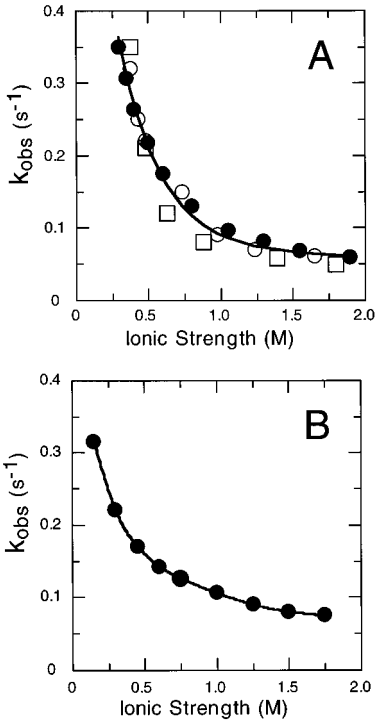

FIGURE 4: Effect of ionic strength on CheY phosphorylation kinetics. CheY (2 μM final concentration) was mixed with 100 mM phosphodonor in the presence of a range of salt concentrations. The apparent first-order rate constant for the exponential approach to steady state (k_{obs}) was determined as in Figure 1. (A) Results obtained with acetyl phosphate. (B) Results obtained with potassium phosphoramidate. Symbols indicate use of different salts to obtain the indicated total ionic strength levels: (●) potassium chloride; (○) potassium glutamate; (□) sodium chloride.

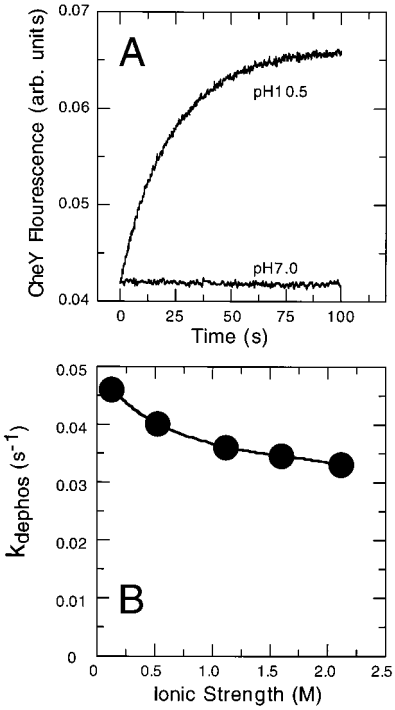

FIGURE 5: pH−jump experiment to monitor CheY dephosphorylation kinetics. (A) A solution containing 20 μM CheY and 50 mM phosphoramidate in dilute buffer (5 mM Tris, 10 mM $MgCl_2$, pH 7.0) was introduced into one drive syringe of the stopped-flow spectrofluorometer. Concentrated buffer (0.2 M unneutralized Tris base or 50 mM Tris, pH 7.0) containing 50 mM phosphoramidate and 10 mM $MgCl_2$ was placed in the second syringe. The contents of the two drive syringes were then mixed 1:1 in the mixing chamber of the stopped-flow instrument, and the ensuing change in CheY fluorescence emission intensity was monitored. The pH resulting from mixing of the CheY/phosphoramidate sample with the high-pH Tris sample was 10.5. Analysis of the time course generated with this mixture indicated a first-order rate constant of 0.046 s^{-1}. Time courses shown represent the average of data generated by 5 consecutive 'shots'. (B) k_{dephos} values were determined as in panel A but over a range of ionic strength values (adjusted by adding KCl to the reaction mixtures).

advantage of the pH dependence of the CheY phosphorylation reaction when phosphoramidate serves as phosphodonor (*40*). The rate of this reaction is negligible at pH values higher than ~9.5. We generated a mixture of CheY and phosphoramidate in dilute buffer poised at neutral pH (where CheY phosphorylation readily occurs); this mixture was jumped rapidly to high pH by mixing with concentrated, high-pH buffer. This generated a solution containing P-CheY at sufficiently high pH (10.5) to effectively shut off any subsequent CheY phosphorylation. pH-jumps were performed in a stopped-flow spectrofluorometer, enabling us to monitor the time course of P-CheY dephosphorylation as reflected by the increase in CheY intrinsic fluorescence that followed the pH up-jump (Figure 5A). The time course of this fluorescence increase followed a single exponential that defined the first-order rate constant for CheY autodephosphorylation (k_{dephos}). The same value of k_{dephos} was obtained at several different concentrations of phosphoramidate (5 mM, 10 mM, 25 mM) and was unaffected by the inclusion of phosphoramidate in the high-pH buffer. This same pH-jump experiment was performed using buffer solutions containing a range of potassium chloride concentrations, and the results indicated a very small dependence of k_{dephos} on ionic strength (Figure 5B). We concluded that the effect of ionic strength on k_{obs} in Figure 4A,B arose primarily from a significant effect on the kinetics of the CheY phosphorylation reaction; it was not due to the relatively minor influence on CheY autodephosphorylation.

These pH−jump experiments provided our most accurate estimates of k_{dephos}. We used the appropriate value from Figure 5B (e.g., $k_{dephos} = 0.034$ s^{-1} at $I = 1.6$ M) for the analysis presented in Figure 2B and Table 1. Previous work (*40*) indicated that k_{dephos} is not sensitive to pH over the range 5−10, and we have confirmed this finding (results not shown).

The k_{obs} values plotted in Figure 4A,B were influenced by both K_s and k_{phos}. Therefore, either or both of these kinetic parameters could be sensitive to ionic strength to generate the observed effect. We examined the individual effects of ionic strength on K_s and k_{phos} for two representative phosphodonors, acetyl phosphate and phosphoramidate. Our results (Figure 6A,B) indicated that k_{phos} decreased as ionic strength increased and that the affinity of CheY for phosphodonor increased (i.e., K_s decreased) as ionic strength increased. The magnitudes of these effects were fairly large. For example, with acetyl phosphate as substrate, an increase in ionic strength from 0.8 to 1.6 resulted in a 10-fold decrease in k_{phos} and a more than a 6-fold decrease in K_s. At lower ionic strengths (e.g., $I < 0.4$ M for acetyl phosphate or $I < 0.8$ M for phosphoramidate), the K_s values became so high that the double-reciprocal plots (Figure 6A,B) appeared to pass through the origin. In other words, at low ionic strength the CheY phosphorylation reaction behaved like a simple second-order reaction with no indication of saturation

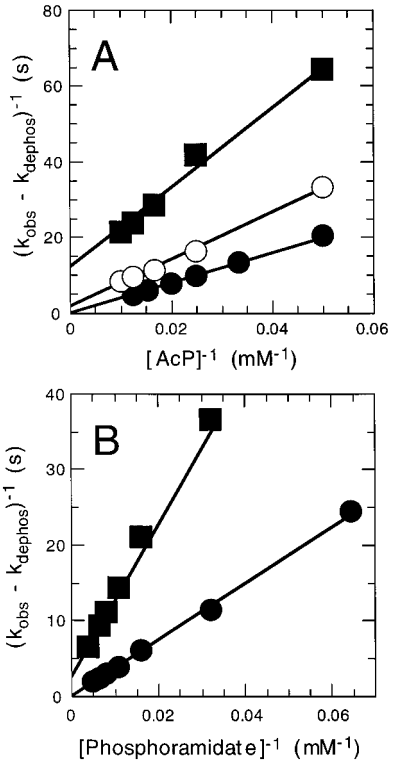

FIGURE 6: Analysis of the effect of ionic strength on CheY phosphorylation kinetics using acetyl phosphate (A) and potassium phosphoramidate (B) as phosphodonors. Data were collected as in Figure 1 and analyzed as in Figure 2. Symbols indicate results obtained at different ionic strength levels (adjusted using KCl): (■) $I = 1.6$; (○), $I = 0.8$; (●) $I = 0.4$.

behavior at even the highest phosphodonor concentration. Using the results of Figure 6 and similar experiments at intermediate ionic strengths, we defined the ionic strength dependence of K_s and k_{phos} (Figure 11). We defer further consideration of these results to the Discussion section.

Effect of pH on CheY Phosphorylation Kinetics. Silversmith et al. (*40*) found that the reaction between CheY and small-molecule phosphodonors exhibits a pronounced pH dependence when the phosphodonor is a protonatable phosphoamide (e.g., phosphoramidate, phosphoimidazole, or phosphohistidine), but not when the phosphodonor is an acyl phosphate (e.g., acetyl phosphate). These results indicate that the protonated phosphoamide is an effective phosphodonor for CheY, but the unprotonated phosphoamide is not. Such experiments were performed before the effect of ionic strength on CheY phosphorylation was appreciated, and so we investigated whether similar experiments carried out at balanced ionic strength would confirm these conclusions. Our results were in complete agreement with those of Silversmith et al. (*40*). Specifically, we found that: (i) the reaction of CheY with acetyl phosphate and other acyl phosphates was insensitive to pH in the range between 5.5 and 10; and (ii) the rate of CheY phosphorylation by phosphoramidate became progressively slower as the pH was increased in the range between 6.5 and 9 (data not shown). We extended analysis of this pH dependence by investigating whether pH influenced k_{phos}, K_s, or both. Our results (Figure 7A) indicate that k_{phos} is affected by pH while K_s is not. This finding confirms a conclusion made by Silversmith et al. (*40*) following different reasoning.

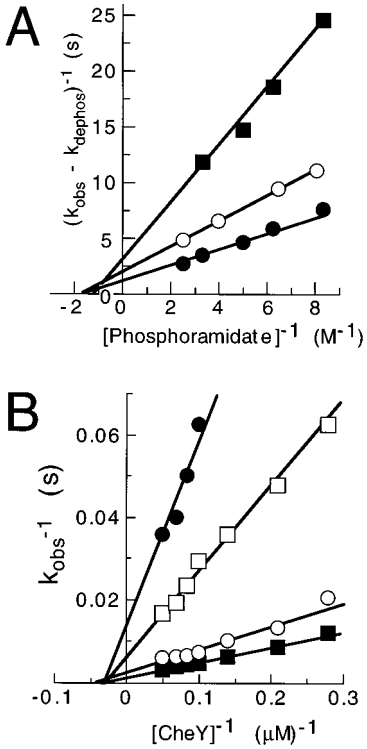

FIGURE 7: Analysis of the effect of pH on CheY phosphorylation kinetics. Panel A: CheY phosphorylation time courses, with potassium phosphoramidate as phosphodonor, were monitored as in Figure 1 and analyzed as in Figure 2 for reactions carried out at pH 6.0 (●), pH 7.5 (○), and pH 8.5 (■), in buffer (0.1 M bis-tris propane, 0.1 M MES) containing sufficient KCl to balance ionic strength at 1.6 M. Panel B: Time courses for CheA→CheY phosphotransfer were monitored as in Figure 8A and analyzed as in Figure 8C for reactions carried out at pH 7.5 (■), pH 8.8 (○), pH 9.3 (□), and pH 10.0 (●) in buffer (0.1 M bis-tris propane or 0.1 M CHES) containing sufficient KCl to balance ionic strength at 0.32 M. The lines in both panels represent computer-generated best fits of the data assuming a linear relationship; these fits included data not included in the figure for the sake of clarity.

Kinetics of Phosphotransfer from P-CheA to CheY. In previous work (*41*) we demonstrated that transfer of phosphate from ^{32}P-CheA to CheY is very rapid and that monitoring this transfer required use of a rapid mixing/quenching apparatus to collect samples over a time course of less than 50 ms. Here, we sought to monitor this reaction by following the change in CheY intrinsic fluorescence associated with CheY phosphorylation. Upon mixing P-CheA with CheY in a stopped-flow spectrofluorometer, we observed a rapid and reversible decrease in the fluorescence emission signal. The time courses presented in Figure 8A illustrate the very rapid, single-exponential decrease in fluorescence that occurred during the first 20 ms after mixing, and this was followed, over the following 50−100 s, by a relatively slow, single-exponential return of the fluorescence signal to a level corresponding to that expected for unphosphorylated CheY (Figure 8B). Analysis of these fluorescence changes is complicated by several factors: (i) both CheA and CheY contribute to the observed fluorescence signal; (ii) CheY intrinsic fluorescence is significantly quenched upon binding to CheA (*51*). We sought to establish that the rapid changes in fluorescence observed in Figure 8 could be used to monitor changes in the concentration of P-CheY in a manner similar to that used above to monitor CheY

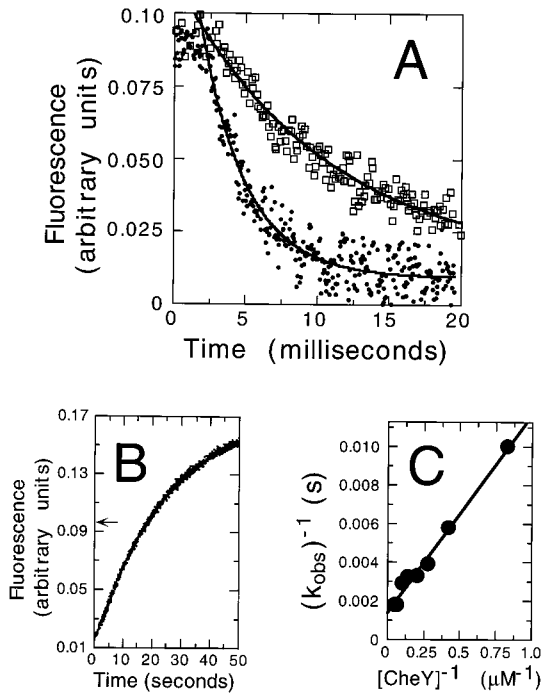

FIGURE 8: Analysis of the time course of fluorescence changes following mixing of P-CheA with CheY. Panel A: 0.15 μM P-CheA was mixed with 1.2 μM CheY (□) or 4.8 μM CheY (●) (concentrations indicate levels present after mixing), and the rapid decrease of fluorescence emission intensity was monitored. The buffer for these experiments was TMD containing 50 mM KCl. Each data set represents the average of 10 consecutive stopped-flow shots. Solid lines represent computer-generated best fits of the data to a single-exponential, and the first-order rate constants derived from such fits were defined as the k_{obs} values; data collected during the first 2 ms of these time courses were not included in such fits because they reflect flow of material into the observation chamber. Panel B: The time course of the reaction between 0.15 μM P-CheA and 1.2 μM CheY was monitored over an extended time scale. The arrow indicates the fluorescence intensity observed at the first measurable time point following mixing (deadtime ~2 ms); on this time scale, the rapid fluorescence decrease depicted in panel A is so compressed that it lies on top of the *y*-axis and so cannot be seen. A computer-generated single-exponential fit of the time course of the slow fluorescence increase generated a curve that overlaid the data completely (and therefore cannot be seen) and indicated a first-order rate constant of 0.04 s^{-1}. Identical results were obtained on this time scale for the reaction using 4.8 μM CheY. Panel C: analysis of the effect of CheY concentration on k_{obs} of the rapid fluorescence decrease. From eq 2, it follows that the *y*-axis intercept of this double-reciprocal plot indicates the value of k_{phos} (750 s^{-1}) and the ratio of the slope to the *y*-axis intercept defines K_s^{P-CheA} (7 μM).

phosphorylation by small-molecule phosphodonors. Control experiments demonstrated that the fluorescence emission signal of CheA was not affected by phosphorylation (results not shown) and indicated that the fluorescence changes associated with CheY binding to unphosphorylated CheA were extremely rapid such that they were complete within the 2 ms deadtime of the stopped-flow instrument (data not shown). Thus, the observed fluorescence changes observed during the first 20 ms of Figure 8A appeared to result from phosphorylation of CheY by P-CheA, and the slow increase in fluorescence over the next 50−100 s (Figure 8B) appeared to represent dephosphorylation of the P-CheY generated during the very rapid reaction. This interpretation was supported by several results described in the following paragraph.

We mixed P-CheA (0.15 μM) with CheY (concentrations ranging from 1.2 to 20 μM) and monitored the time course of the fluorescence changes. Analysis of these results (Figure 8C) indicated that the rate of the reaction taking place in the fast phase (responsible for the observed fluorescence decrease, as in Figure 8A) was affected by the CheY concentration in a saturable manner. By contrast, the rate of the slow phase (fluorescence increase, as in Figure 8B) was not sensitive to CheY concentration (results not shown). Further analysis of the fast-phase kinetics indicated a K_s value of 7 ± 2 μM for the putative P-CheA·CheY complex and an extrapolated first-order rate constant (k_{phos}) value of 750 ± 100 s^{-1} at saturating CheY concentration (Figure 8C). These values match very well with those determined previously (*41*) from quenched-flow experiments (K_s = 6.5 ± 2 μM, k_{phos} = 650 ± 200 s^{-1}) performed under identical conditions. The first-order rate constant measured for the slow fluorescence increase (0.04 s^{-1}) (Figure 8B) also matches well with that expected for autodephosphorylation of P-CheY (*24*, *25*, *40*, *41*).

Results presented in preceding sections indicated that the rate of CheY phosphorylation by small-molecule phosphodonors was sensitive to ionic strength and, with some phosphodonors, to pH. We investigated the effect of these conditions on the kinetics of phosphotransfer from P-CheA to CheY by making use of the spectrofluorometric assay described in the preceding paragraphs.

As shown in Figure 9A, ionic strength conditions had a significant effect on the observed rate of CheA→CheY phosphotransfer. Increasing concentrations of potassium chloride and potassium glutamate were equally effective in decreasing the rate of this reaction. Analysis of experiments conducted at a series of CheY concentrations and at a series of salt concentrations indicated that the primary influence of increased ionic strength was to increase the K_s of the P-CheA·CheY complex and that the rate of phosphotransfer within this complex (k_{phos}) was relatively insensitive to ionic strength (Figure 9B). Graphical representations of the effect of ionic strength on K_s^{P-CheA} and $k_{phos}^{A\rightarrow Y}$ are shown in Figure 11 and point out that these effects differ from those observed for the reaction of CheY with small-molecule phosphodonors. We defer further consideration of Figure 11 and these differences to the Discussion section.

As shown in Figure 7B, pH also had a significant effect on the kinetics of CheA→CheY phosphotransfer, and this effect resulted from pH influencing the value of k_{phos}. By contrast, pH had no significant effect on K_s^{P-CheA} (Figure 7B). These results are very similar to the pH sensitivity observed for phosphorylation of CheY by small-molecule phosphodonors (Figure 7A) and confirm results reported previously by Silversmith et al. (*40*).

Effect of CheA on CheY Phosphorylation by Small-Molecule Phosphodonors. The value of k_{phos} for CheA→CheY phosphotransfer is much larger than the corresponding value for CheY phosphorylation by any of the small-molecule phosphodonors. In view of this difference, we explored the possibility that binding of CheY to CheA might be able to accelerate CheY phosphorylation by small-molecule phosphodonors. We examined the reaction of CheY with acetyl phosphate and phosphoramidate in the presence of $CheA^{124-257}$. This CheA fragment corresponds to the P2 segment of CheA (*44*) and encompasses the CheY binding site (*51*) but lacks

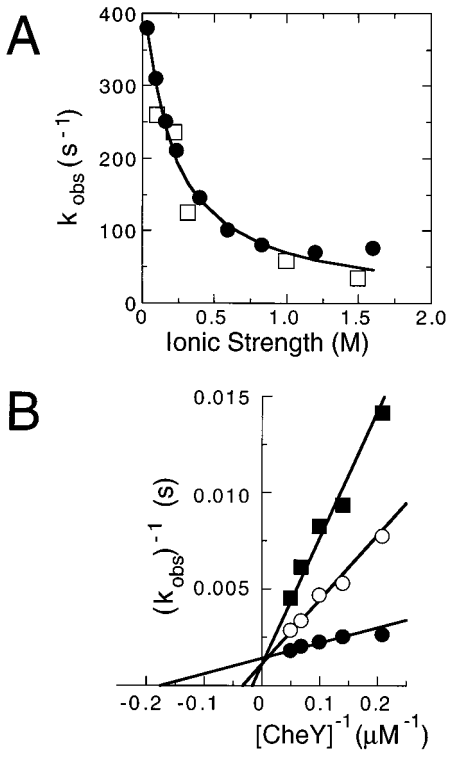

FIGURE 9: Effect of ionic strength on the kinetics of the CheA→CheY phosphotransfer reaction. Panel A: CheY (4.8 μM final concentration) was mixed with 0.15 μM P-CheA in the presence of a range of salt concentrations in 10 mM Tris buffer, pH 7.5. The apparent first-order rate constant for the exponential approach to steady state (k_{obs}) was determined as in Figure 8A. Symbols indicate use of different salts to obtain the indicated total ionic strength levels: (●) potassium chloride; (□) potassium glutamate. Panel B: Analysis of the effect of ionic strength on CheA→CheY phosphotransfer kinetics. Data were collected as in Figure 8A and analyzed as in Figure 8C. Symbols indicate results obtained at different ionic strength levels (adjusted using KCl): (●) $I = 0.038$ M, (○) $I = 0.35$ M, (■) $I = 1.6$. The double-reciprocal plot indicates that the *y*-axis intercept $(k_{phos})^{-1}$ is relatively unaffected by ionic strength, while the value of the *x*-axis intercept $(K_s^{P-CheA})^{-1}$ becomes significantly lower as ionic strength is increased. The lines represent computer-generated best fits of the data assuming a linear relationship; these fits included data not included in the figure for the sake of clarity.

the region of CheA that contains the phosphorylation site as well as the region of the protein containing the kinase active site (*30*). This CheA fragment binds CheY with approximately the same affinity as does full-length CheA (*52*), and its use simplified analysis of fluorescence data because it lacks tryptophan residues. We found that $CheA^{124-257}$ inhibited CheY phosphorylation by either phosphoramidate (Figure 10) or acetyl phosphate (data not shown) as phosphodonor.

DISCUSSION

The initial observations that CheY and other response regulators can become phosphorylated by acquiring a phosphoryl group directly from numerous small-molecule phosphodonors changed how we think about these proteins (*26*, *36*−*38*). Previously thought of as passive 'traditional substrates' for their respective cognate sensor kinases, CheY and other response regulators are now thought of as enzymes that catalyze transfer of a phosphoryl group (*16*, *36*) from a variety of different phosphodonors (e.g., P-CheA or a small-

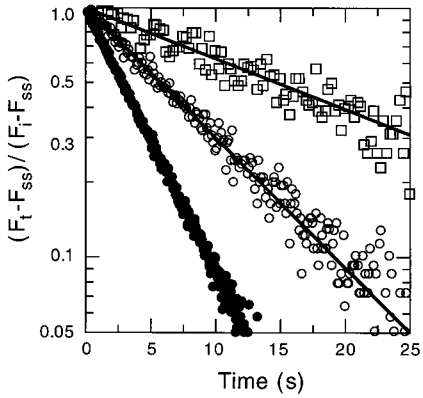

FIGURE 10: Effect of $CheA^{124-257}$ on CheY phosphorylation kinetics. Reaction mixtures contained 10 μM CheY, 100 mM phosphoramidate, and (●) no $CheA^{124-257}$, (○) 2 μM $CheA^{124-257}$, or (□) 13 μM $CheA^{124-257}$ in TMD buffer containing 50 mM KCl. Reaction time courses were monitored using fluorescence emission changes and plotted in normalized semilog fashion as in Figure 1B. Time courses shown represent the average of data generated by 4 or 5 consecutive 'shots'.

molecule phosphodonor) to the conserved Asp residue located in the 'acid pocket' (*32*−*35*) at the active site of the receiver module. This raises the following question: Is P-CheA just another 'passive' phosphodonor for CheY, or does P-CheA contribute to catalysis of CheY phosphorylation in a manner not possible for small-molecule phosphodonors? In addition to stimulating discussion of such fundamental questions, the discovery of CheY phosphorylation by small-molecule phosphodonors has provided a very useful method for generating relatively large populations of phosphorylated CheY, and this has enabled key experiments to define some of the structural and activity changes associated with phosphorylation (*18*, *53*). When utilizing this method for generating P-CheY, it would be helpful to have a firm grasp on the kinetic parameters that govern the rate of CheY phosphorylation by small-molecule phosphodonors. In initiating our kinetic analysis of CheY phosphorylation, we sought to define these basic kinetic parameters as well as to compare the kinetics of the CheY phosphorylation by small-molecule phosphodonors to the kinetics of the CheA→CheY phosphotransfer reaction.

We investigated the kinetics of CheY phosphorylation utilizing a variety of different small-molecule phosphodonors. Our results make several significant contributions to understanding this reaction: (i) they help to define the minimal reaction scheme that describes CheY phosphorylation by small-molecule phosphodonors and provide experimental support for this model over possible alternatives; (ii) they define the values of the basic kinetic parameters (K_s and k_{phos}) that govern CheY phosphorylation by several phosphodonors; (iii) they establish that CheY phosphorylation by small-molecule phosphodonors is significantly slower than CheY phosphorylation directed by CheA, even at phosphodonor concentrations approaching 0.1 M; (iv) they establish how ionic strength and pH influence the kinetics of CheY phosphorylation by P-CheA and small-molecule phosphodonors. The potential significance of these results with respect to the catalytic mechanism of CheY phosphorylation is discussed below.

The reaction scheme that best accounts for our kinetic results is depicted in eq 1: for the interaction of CheY with

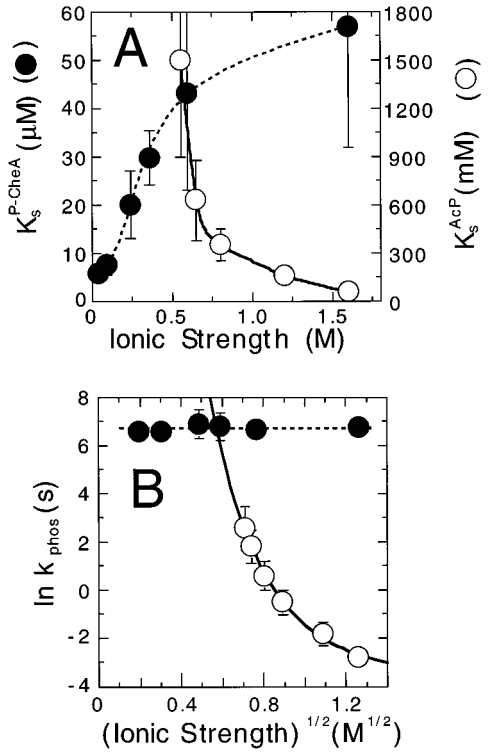

FIGURE 11: Effect of ionic strength on k_{phos} and K_s for the CheA→CheY phosphotransfer reaction and for CheY phosphorylation by AcP. The results shown here include those from Figures 6A and 9B and from similar experiments conducted at a series of ionic strength levels obtained by addition of KCl. Panel A: The effect of ionic strength on K_s for the P-CheA·CheY complex (●) and K_s for the CheY·AcP complex (○). The solid and dashed lines connecting the data points in this panel were added to help the reader to distinguish between the two data sets and have no theoretical significance. Panel B: The effect of ionic strength on k_{phos} for the P-CheA·CheY complex (●) and for the CheY·AcP complex (○). The solid line shows the best fit of the Watkins "parallel plate" model (*55*) to the data obtained for the reaction of CheY with AcP. This fit uses an equation that considers only monopole-monopole interactions: $\ln k(I) = \ln k_\infty - V_{ii}\cdot X(I)$. Parameters obtained from the fit are: $\ln k_\infty = -3.514$, $V_{ii} = -79.09$, and $\rho = 8.63$ Å. The equation and symbols are those defined in Watkins et al. (*55*). Error bars represent standard errors reported by the linear least-squares fitting program of SigmaPlot using a single set of data (such as in Figure 2B or Figure 8C) for each ionic strength.

small-molecule phosphodonors, our results indicate low-affinity binding of phosphodonor to CheY, followed by relatively slow, irreversible phosphotransfer from the donor to Asp^{57} of CheY, followed by slow autodephosphorylation of P-CheY. This basic scheme was utilized previously by Lukat et al. (*36*) and Silversmith et al. (*40*) in analyzing the effect of phosphodonor concentration on the steady-state level of P-CheY. Although this simple scheme is certainly a common one for analyzing enzyme−substrate interactions, there are other equally simple schemes (*50*) that could have accounted for the experimental results gathered prior to our studies. By conducting detailed kinetic studies of CheY phosphorylation using a variety of different phosphodonors, we generated results that argue against such alternatives and that provide experimental support for the basic reaction scheme of eq 1 (discussed under Experimental Procedures).

Previous efforts to characterize the kinetics of CheY phosphorylation by small-molecuule phosphodonors were limited to determining the effect of phosphodonor concentration on the steady-state level of P-CheY (*32*, *40*). By extending our analysis to monitor the rate of approach to this steady state, we were able to define the approximate K_s values for the Michaelis complexes of CheY with several different phosphodonors and to define the value of the limiting rate constant for phosphotransfer within each such complex (k_{phos}). Because we wanted to measure and compare the K_s and k_{phos} values for a variety of different phosphodonors, we chose standard conditions (I = 1.6 M) that enabled us to include measurements made at very high phosphodonor concentrations. For experiments conducted with some of the weakest binding phosphodonors (e.g., phosphoramidate and carbamoyl phosphate), the high ionic strength conditions lowered the K_s values into a measurable range. These K_s values indicate that CheY binds these small molecule phosphodonors relatively weakly. We also note that the affinity of CheY for P-CheA appears to be 200−1000-fold greater than the affinity of CheY for the small-molecule phosphodonors (Table 1).

In previous work (*41*) and in work reported here, we demonstrated that phosphotransfer from P-CheA to CheY occurs very rapidly (k_{phos} = 700−800 s^{-1}). By comparison, the k_{phos} values for small-molecule phosphodonors are very slow (0.06−0.5 s^{-1}). However, it is worth noting that these k_{phos} values were measured under conditions of high ionic strength (for the reasons discussed above). What values of k_{phos} would one expect for the small-molecule phosphodonors at low ionic strength? This question is difficult to answer with great certainty because at low ionic strength we are not able to reach phosphodonor concentrations sufficiently high to begin to see saturation: at low ionic strength, the CheY phosphorylation reaction exhibits a strictly first-order dependence on phosphodonor concentration. With acetyl phosphate, for example, low ionic strength experiments (I = 0.2 M) indicated that $k_{obs} \sim 5\ M^{-1}\ s^{-1} \times$ [AcP] (results not shown). According to this relationship, huge concentrations of phosphodonor (∼0.5 M) would be necessary to drive the CheY phosphorylation reaction at a rate approaching even 1% of the rate expected for the A→Y phosphotransfer reaction [if one assumes an intracellular CheY concentration of ∼10 mM (*1*)]. Such comparisons indicate that, under in vivo conditions [where acetyl phosphate levels can reach only the millimolar range (*33*)], the level of P-CheY generated by CheA-mediated phosphorylation would far outweigh the level of P-CheY generated via CheY phosphorylation by acetyl phosphate.

The value of k_{phos} for CheA→CheY phosphotransfer is at least 1000-fold higher than the fastest k_{phos} value for CheY phosphorylation by small-molecule phosphodonors. This large difference indicates that P-CheA makes significant contributions to catalysis of CheY phosphorylation, contributions that are not possible for the small-molecule phosphodonors. Such contributions might include the following: favorably orienting the geometry of the Asp^{57} carboxylate and the phospho-donating histidine group; providing active site groups to promote specific events of phosphotransfer; fostering binding interactions in the transition state that lower the activation energy of phosphotransfer; providing a general environment [e.g., of low dielectric constant (*57*)] that enhances specific interactions or events (see below). We investigated the possibility that binding of CheY to the P2 module of CheA could enhance the rate of CheY phospho-

rylation by small-molecule phosphodonors. Contrary to such expectations, we observed that the CheA P2 module inhibited this reaction. Crystallographic characterization of the complex formed between CheY and the P2 module (*58*, *59*) indicates that the CheY active site adopts a more 'open' conformation when complexed to $CheA^{124-257}$. Therefore, it seems unlikely that the reduced phosphorylation rate we observed could have resulted from P2 blocking access of small-molecule phosphodonors to the CheY active site. Thus, it appears that in this 'open' conformation, CheY's active site becomes less reactive toward small-molecule phosphodonors. There are CheA sites outside of P2 that must interact with CheY during phosphotransfer (e.g., those in the P1 module that flank the CheA phosphorylation site). We are currently investigating whether such interactions affect CheY phosphorylation by small-molecule phosphodonors and whether mutations at such sites affect the kinetics of phosphotransfer from phospho-CheA to CheY.

The effects of ionic strength on the kinetics of CheY phosphorylation by small-molecule phosphodonors and by phospho-CheA have not been reported previously. It is likely that this sensitivity affected previously published estimates of the K_m values for phosphodonor turnover by CheY (*36*, *40*). Several aspects of this ionic strength effect merit further discussion. First, our results stress the need to consider factors such as salt concentrations when attempting to assess the in vivo significance of results obtained from in vitro experiments. The ionic environment of the *E. coli* cytoplasm is subject to considerable variation in response to the osmolarity of the growth medium (*60*, *61*). Many standard growth media and the motility medium used by workers in the *E. coli* chemotaxis field have an osmolarity of ~0.1 M. For cells experiencing such conditions, the major intracellular cationic component (K^+) and its counterions (e.g., glutamate) would give rise to an effective intracellular ionic strength of ~0.2 M. Buffer solutions containing 0.2 M potassium glutamate (or potassium chloride) are sometimes used for in vitro experiments to mimic in vivo ionic strength conditions (*61*). Using this as a reasonable benchmark for in vivo conditions, our in vitro results (Figure 11) indicate that the most physiologically relevant kinetic parameters for the CheA→CheY phosphotransfer reaction would be $K_s \sim 20\ \mu M$ and $k_{phos} \sim 800\ s^{-1}$. For the reaction of CheY with AcP at $I = 0.2$ M, the relevant quantitative description of the reaction would be a simple second-order reaction with a rate of ~5 $M^{-1}\ s^{-1} \times$ [AcP].

Figure 11A,B shows the effect of ionic strength on k_{phos} and K_s both for the CheA→CheY phosphotransfer reaction and for the interaction of CheY with AcP. The values plotted in this figure were compiled from results presented in Figure 6A and Figure 9B, and from additional experiments conducted at intermediate ionic strength levels (results not shown). Does this information provide any insight into the catalytic mechanism of phosphotransfer from P-CheA to CheY or insight into the mechanism of CheY phosphorylation by small-molecule phosphodonors? In general, the ionic composition of the medium can shield the charges of two interacting reactants. The magnitude of the effects of ionic strength on kinetic constants reflects the magnitude of the charges on the reactants and the signs of these charges (*54*, *55*). Thus, the simplest interpretation of the effect of ionic strength on K_s of the P-CheA·CheY complex is that binding of P-CheA to CheY involves interactions between oppositely charged groups. The crystal structure of a complex between CheY and the P2 module of CheA indicates that several CheY lysine side chains participate in hydrogen-bonding interactions with acidic amino acid side chains of P2 (*58*, *59*). It would not be surprising if such interactions were responsible for the observed effect of ionic strength on K_s^{P-CheA}. In contrast to the ability of increased ionic strength to inhibit binding of CheY to the phosphodonor P-CheA, we observed that the affinity of CheY for small-molecule phosphodonors was increased as the ionic strength increased. The simplest interpretation of this effect is that binding of the small-molecule phosphodonors to the CheY active site must overcome repellent interactions between like charges (such as between the 'acid pocket' carboxylates and the phosphate of the phosphodonor); partial shielding of these charges at higher ionic strength would facilitate binding. If such repulsive interactions affect binding of small-molecule phosphodonors to CheY, one might also expect such repulsive forces to come into play when the phosphorylated histidine of P-CheA interacts with the CheY active site. However, in the P-CheA·CheY complex, CheY is tethered by tight binding to a region (P2) distinct from the CheA phosphorylation site, a situation that would overcome/mask repulsive interactions between the CheY active site and the phosphorylated histidine side chain of the CheA. There is also the possibility that CheA neutralizes or shields groups that otherwise would be capable of repulsive interactions.

Analysis of our results and graphical extrapolation to saturating CheY concentration enabled us to estimate k_{phos}, the rate constant for phosphotransfer within the P-CheA·CheY complex. The value of k_{phos} for CheA→CheY phosphotransfer was not sensitive to ionic strength in the range between 0.04 and 1.6 M. By contrast, the value of k_{phos} estimated for the reaction of CheY with various small-molecule phosphodonors was quite sensitive to ionic strength, decreasing significantly as ionic strength was increased. This result suggests that the phosphotransfer step (from bound phosphodonor to Asp^{57} of CheY) for these reactions involves a rate-promoting interaction between two charges and that this interaction is inhibited as the ionic strength is increased. This might involve, for example, ionic shielding of two oppositely charged groups that approach one another in the transition state; alternatively, if catalysis involves separation of two charged groups, increased ionic strength might affect the active site structure in a manner that inhibits this separation. Interactions between several charged groups are likely to be involved in the phosphotransfer step: nucleophilic attack of the phosphoryl phosphorus by the β-carboxylate of Asp^{57} (*39*); interaction of Mg^{2+} with the carboxylates of Asp^{13} and Asp^{57} (*26*, *33*); interaction of Mg^{2+} with the anionic phosphate oxygens to shield their charges (*56*); and repulsive interactions between the phosphate oxygens and the negative charge of the Asp^{57} carboxylate. In the absence of additional information, it is not possible to know whether one of these interactions (or some combination of them) is responsible for the observed effect of ionic strength on k_{phos}. In fact, it is not possible to specify, with any certainty, the magnitudes of the interacting charges because several features of the active site (e.g., the local dielectric constant and radius of the charge−charge interaction site) dictate how much any charge−charge interaction

can influence a rate constant (*55*). Despite these limitations on quantitative analysis, the general trend shown in Figure 11 suggests that k_{phos} likely continues to increase as ionic strength is decreased. Of course, it would be of great interest to define the value of k_{phos} at even lower ionic strength levels than the lower limit used for the experiments of Figures 6 and 11. Unfortunately, for the reasons discussed above, k_{phos} cannot be determined directly through experimental measurements at lower ionic strength. The question remains: How high might k_{phos} become at very low ionic strength? The relationship shown in Figure 11 (ln k_{phos} versus the square root of the ionic strength) can be analyzed using the Watkins "parallel plate" model of electrostatic interactions (*55*), and the parameters defined by this analysis can be used to extrapolate this plot to lower ionic strength levels. According to this extrapolation, k_{phos} for acetyl phosphate would reach a value of 700 s^{-1} at an ionic strength of ~0.3 M. Although this extrapolation is based on a limited data set and makes several assumptions about how ionic strength affects this reaction, it does raise an interesting possibility: perhaps CheA accelerates phosphotransfer from His^{48}~P to CheY (for which $k_{phos} \sim 700\ s^{-1}$) by providing an environment of relatively low ionic strength. In the context of such an environment, CheY would catalyze phosphotransfer much more rapidly than would be possible for a solvent-exposed CheY active site, and CheA would achieve this acceleration not by providing any specific active site functional groups itself, but rather by providing a general environment in which the basic active site machinery of CheY could operate more rapidly. As indicated by the results presented in Figure 11, this would not require extreme changes in the CheY active site: a relatively subtle shift in the dielectric environment could have a pronounced effect on the rate of CheY phosphorylation. Our observation that k_{phos} for phosphotransfer from P-CheA to CheY is insensitive to ionic strength is consistent with the possibility that CheA might provide a relatively 'shielded' environment in which the CheY active site can operate, but strong support for such an arrangement will require detailed structural information about the P-CheA·CheY complex. Clearly, much remains to be learned about how the CheY active site catalyzes phosphotransfer from small-molecule phosphodonors as well as about how this active site operates in the context of a P-CheA·CheY complex.

ACKNOWLEDGMENT

We thank R. VanBruggen for expert technical assistance and J. S. Parkinson for providing invaluable *E. coli* strains and plasmids. We also thank Stephan Scuhster and R. Silversmith and R. Bourret for sharing their results prior to publication as well as for stimulating discussions.

REFERENCES

1. Stock, J., and Surette, M. G. (1996) in *Escherichia coli and Salmonella. Cellular and Molecular Biology* (Neidhardt, F. C., Ed.) pp 1103−1129, ASM Press, Washington, D.C.
2. Eisenbach, M. (1996) *Mol. Microbiol. 20*, 903−910.
3. Berg, H. C., and Anderson, R. A.. (1973) *Nature 245*, 380−382.
4. Silverman, M., and Simon, M. (1974) *Nature 249*, 73−74.
5. Macnab, R. M. (1996) in *Escherichia coli and Salmonella. Cellular and Molecular Biology* (Neidhardt, F. C., Ed.) pp 123−145, ASM Press, Washington, D.C.
6. Larsen, S. H., Reader, R. W., Kort, E. N., Tso, W.-W., and Adler, J. (1974) *Nature 249*, 74−77.
7. Macnab, R. M., and Koshland, D. E., Jr. (1972) *Proc. Natl. Acad. Sci. U.S.A. 69*, 2509−2512.
8. Berg, H. C., and Brown, D. A. (1972) *Nature 239*, 500−504.
9. Dahlquist, F. W., Lovely, P., and Koshland, D. E., Jr. (1972) *Nature (London), New Biol. 236*, 120−123.
10. Parkinson, J. S., Parker, S. R., Talbert, P. B., and Houts, S. E. (1983) *J. Bacteriol. 155*, 265−274.
11. Clegg, D. O., and Koshland, D. E., Jr. (1984) *Proc. Natl. Acad. Sci. U.S.A. 81*, 5056−5060.
12. Wolfe, A. J., Conley, M. P., Kramer, T. J., and Berg, H. C. (1987) *J. Bacteriol. 169*, 1878−1885.
13. Welch, M., Oosawa, K., Aizawa, S.-I., and Eisenbach, M. (1993) *Proc. Natl. Acad. Sci. U.S.A. 90*, 8787−8791.
14. Ravid, S., Matsumura, P., and Eisenbach, M. (1986) *Proc. Natl. Acad. Sci. U.S.A. 84*, 7157−7161.
15. Barak, R., and Eisenbach, M. (1992) *Biochemistry 31*, 1821−1826.
16. Sanders, D. A., Gillece-Castro, B. L., Stock, A. M., Burlingame, A. L., and Koshland, D. E., Jr. (1989) *J. Biol. Chem. 264*, 21770−21778.
17. Bourret, R. B., Hess, J. F., and Simon, M. I. (1990) *Proc. Natl. Acad. Sci. U.S.A. 87*, 41−45.
18. Welch, M., Oosawa, K., Aizawa, S.-I., and Eisenbach, M. (1994) *Biochemistry 33*, 10470−10476.
19. Hess, J. F., Oosawa, K., Matsumura, P., and Simon, M. I. (1987) *Proc. Natl. Acad. Sci. U.S.A. 84*, 7609−7613.
20. Hess, J. F., Bourret, R. B., and Simon, M. I. (1988b) *Nature 336*, 139−143.
21. Borkovich, K. A., Kaplan, N., Hess, J. F., and Simon, M. I. (1989) *Proc. Natl. Acad. Sci. U.S.A. 86*, 1208−1212.
22. Borkovich, K. A., and Simon, M. I. (1990) *Cell 63*, 1339−1348.
23. Ninfa, E. G., Stock, A., Mowbray, S., and Stock, J. (1991) *J. Biol. Chem. 266*, 9764−9770.
24. Hess, J. F., Bourret, R. B., Oosawa, K., Matsumura, P., and Simon, M. I. (1988) *Cold Spring Harbor Symp. Quant. Biol. 53*, 41−48.
25. Hess, J. F., Oosawa, K., Kaplan, N., and Simon, M. I. (1988) *Cell 53*, 79−87.
26. Stock, J. B., Surette, M. G., Levit, M., and Park, P. (1995) in *Two-Component Signal Transduction* (Hoch, J. A., and Silhavy, T. J., Eds.) pp 25−561, ASM Press, Washington, D.C.
27. Lukat, G. S., Lee, B. H., Mottonen, J. M., Stock, A. M., and Stock, J. B. (1991) *J. Biol. Chem. 266*, 8348−8354.
28. Sanna, M. G., Swanson, R. V., Bourret, R. B., and Simon, M. I. (1995) *Mol. Microbiol. 15*, 1069−1079.
29. Huang, C. X., and Stewart, R. C. (1993) *Biochim. Biophys. Acta 1202*, 297−304.
30. Parkinson, J. S., and Kofoid, E. C. (1992) *Annu. Rev. Genet. 26*, 71−112.
31. Chang, C., and Stewart, R. C. (1998) *Plant Physiol. 117*, 723−732.
32. Stock, A. M., Mottonen, J. M., Stock, J. B., and Schutt, C. E. (1989) *Nature 337*, 745−749.
33. Stock, A. M., Martinez-Hackert, E., Rasmussen, B. F., West, A. H., Stock, J. B., Ringe, D., and Petsko, G. A. (1993) *Biochemistry 32*, 13375−13380.
34. Volz, K., and Matsumura, P. (1991) *J. Biol. Chem. 266*, 15511−15519.
35. Moy, F. J., Lowry, D. F., Matsumura, P., Dahlquist, F. W., Krywko, J. E., and Domaille, P. J. (1994) *Biochemistry 33*, 10731−10742.
36. Lukat, G. S., McCleary, W. R., Stock, A. M., and Stock, J. B. (1992) *Proc. Natl. Acad. Sci. U.S.A. 89*, 718−722.
37. McCleary, W. R., and Stock, J. B. (1994) *J. Biol. Chem. 269*, 31567−31572.
38. Zaph, J. W., Hoch, J. A., and Whitely, J. M. (1996) *Biochemistry 35*, 2926−2933.
39. Lukat, G. S., Stock, A. M., and Stock, J. B. (1990) *Biochemistry 29*, 5436−5442.
40. Silversmith, R. E., Appleby, J. L., and Bourret, R. B. (1997) *Biochemistry 36*, 14965−14974.

41. Stewart, R. C. (1997) *Biochemistry 36*, 2030−2040.
42. Wolfe, A. J., and Stewart, R. C. (1993) *Proc. Natl. Acad. Sci. U.S.A. 90*, 1518−1522.
43. Gill, S. C., and von Hippel, P. H. (1989) *Anal. Biochem. 182*, 319−326.
44. Morrison, T. B., and Parkinson, J. S. (1994) *Proc. Natl. Acad. Sci. U.S.A. 91*, 5485−5489.
45. Lipmann, F., and Tuttle, L. C. (1945) *J. Biol. Chem. 159*, 21−28.
46. Camici, G., Manao, G., Cappugi, G., and Ramponi, G. (1976) *Experientia 32*, 535−536.
47. Paoli, G., Camici, G., Manao, G., and Ramponi, G. (1995) *Experientia 51*, 57−62.
48. Sheridan, R. C., McCullough, J. F., and Wakefield, Z. T. (1972) *Inorg. Synth. 13*, 23−26.
49. Bevington, P. R. (1969) in *Data Reduction and Error Analysis for the Physical Sciences*, McGraw-Hill, New York.
50. Strickland, S., Palmer, G., and Massey, V. (1975) *J. Biol. Chem. 250*, 4048−4052.
51. Swanson, R. V., Lowry, D. F., Matsumura, P., McEvoy, M. M., Simon, M. I., and Dahlquist, F. W. (1995) *Nat. Struct. Biol. 2*, 906−910.
52. Li, J., Swanson, R. V., Simon, M. I., and Weis, R. M. (1995) *Biochemistry 34*, 14626−14636.
53. Lowry, D. F., Roth, A. F., Rupert, P. B., Dahlquist, F. W., Moy, F. J., Domaille, P. J., and Matsumura, P. (1994) *J. Biol. Chem. 269*, 26358−26362.
54. Debye, P. (1942) *Trans. Electrochem. Soc. 82*, 265−272.
55. Watkins, J. A., Cusanovich, M. A., Meyer, T. E., and Tollin, G. (1994) *Protein Sci. 3*, 2104−2114.
56. Herschlag, D., and Jencks, W. P. (1990) *J. Am. Chem. Soc. 112*, 1942−1950.
57. Shan, S.-O., and Herschlag, D. (1996) *Proc. Natl. Acad. Sci. U.S.A. 93*, 14474−14479.
58. McEvoy, M. M., Hausrath, A. C., Randolph, G. B., Remington, S. J., and Dahlquist, F. W. (1998) *Proc. Natl. Acad. Sci. U.S.A. 95*, 7333−7338.
59. Welch, M., Chinardet, N., Mourey, L., Birck, C., and Samama, J.-P. (1998) *Nat. Struct. Biol. 5*, 25−29.
60. Record, M. T., Jr., Courtenay, E. S., Caylery, D. S., and Guttman, H. J. (1998) *Trends Biochem. Sci. 23*, 143−148.
61. Richey, B., Cayley, D. S., Mossing, M. C., Kolka, C., Anderson, C. F., Farrar, T. C., and Record, M. T., Jr. (1987) *J. Biol. Chem. 262*, 7157−7164.

BI981707P